

Photoenhanced Catalytic Dehydrogenation of Propan-2-ol with Homogeneous Rhodium-Tin Complexes

By Hiroshi Moriyama, Toshiya Aoki, Sumio Shinoda, and Yasukazu Saito,* Institute of Industrial Science, University of Tokyo, 22-1, Roppongi 7 Chome, Minato-ku, Tokyo 106, Japan

The effect of photoirradiation was investigated for the catalytic dehydrogenation of propan-2-ol with homogeneous rhodium-tin complexes. A large reduction of activation energy from 117 to 11 kJ mol⁻¹ was observed. The wavelength dependence of quantum efficiency showed that it exceeded unity in the u.v. region with an appropriate catalyst composition. A mechanism is proposed, in which the generation of co-ordinatively unsaturated catalytically active species by the photocleavage of the Rh-Sn co-ordination bond is assumed. Photocatalysis in endothermic reactions is discussed from the viewpoint of solar energy storage.

THE photogeneration of catalytically active species in homogeneous organic reactions has become of interest in recent years.¹⁻³ Sometimes the effect of photoirradiation is so large that a high quantum efficiency (Φ) is observed, *e.g.*, Φ 429 for the isomerization of pent-1-ene to pent-2-enes with Fe(CO)₅.^{4,5} Recently, Φ 0.9 was attained by the combined use of a photosensitizer (benzophenone) and a catalyst (colloidal platinum) for the dehydrogenation of propan-2-ol.⁶ This reaction [equation (1)] is important, as it forms an energy-storing process (ΔH° 55.2 and ΔG° 32 kJ mol⁻¹ for the pure liquids).^{6,7}



We have reported in a preliminary paper⁸ that photoirradiation markedly enhances reaction (1) catalysed by homogeneous rhodium-tin complexes,⁹ with Φ exceeding unity in the u.v. region. Investigation of wavelengths up to the visible region (<700 nm) also seemed attractive. In the present paper, we give extensive surveys of this photocatalytic system and discuss the mechanism of the photoactivation of the catalyst.

EXPERIMENTAL

Preparation of the Catalyst Solution.—Reagent grade RhCl₃·3H₂O, SnCl₂·2H₂O, and LiCl were used without further purification. Propan-2-ol was dried over CaO and distilled before use. Appropriate amounts of RhCl₃·3H₂O, SnCl₂·2H₂O, and LiCl were dissolved in propan-2-ol at 0 °C with stirring under nitrogen, until the solution became homogeneous and wine-red in colour.

Procedure.—The solution (200 ml) was deaerated by bubbling with nitrogen gas in the photochemical reactor before reaction. The reactor was equipped with a thermometer and a reflux condenser to which a gas burette (500 ml) was attached. After refluxing of the solution became stable, irradiation was started with low-pressure mercury lamps (Wako Denki Co. Ltd.; LP-10D type; 3 × 24 W) through a quartz-glass vessel put inside the reactor. The volume of the evolved gas was measured at the atmospheric pressure as a function of time. The reaction temperature was controlled within ±0.1 °C. After the reaction was stopped, the amount of acetone was determined by g.l.c. (stationary phase PEG 1000) and ¹H n.m.r. spectroscopy

(Hitachi R-20B). The composition of the gas phase was analysed by g.l.c. (stationary phase MS-5A).

Unirradiated reactions were carried out in 200 ml three-necked round-bottomed flasks, with the solution (100 ml) degassed by freeze-pump-thaw cycles. The reaction procedure was the same as that of the photoirradiated ones.

The dependence of the quantum efficiency on the wavelength was determined with a spectrophotometric reactor (Jasco CRM-FA; diffraction grating type; 2 kW Xe arc-lamp), comparing the amount of acetone formed with the number of absorbed photons. The wavelength of 208–696 nm was divided into twenty parts at equal intervals, for each of which was set a standard 1-cm pathlength quartz cell containing 3.0 ml of the solution. The temperature was maintained at 20 ± 0.1 °C.

The electronic absorption spectra were measured with a photometric spectrometer (Beckman 25) at ambient temperature. Pulsed Fourier transform n.m.r. spectra were recorded on JEOL JNM-FX 60 and JNM-FX 90Q spectrometers operating at 59.80 MHz for ¹H and 33.34 MHz for ¹¹⁹Sn (multi-tunable probe), respectively. Chemical shifts are given relative to the external Si(CH₃)₄ and Sn(CH₃)₄ references, respectively, where a negative sign indicates a shift to higher field.

RESULTS

The evolution of hydrogen was proportional to time elapsed under photoirradiation, as shown typically in Figure 1, leading to the equimolar formation of acetone. When the irradiation was turned off, only very low thermocatalytic activity was observed. Upon illumination, however, the activity was enhanced. It was found that the presence of tin(II) chloride was necessary (typically [SnCl₂]:[RhCl₃] ≥ 1.5) to prevent the precipitation of metallic rhodium.

Figure 2 shows the dependence of the initial rates on the catalyst concentration, with the fixed ratios of [SnCl₂]:[RhCl₃] = 3.5 and [LiCl]:[RhCl₃] = 3.0. If the contribution from the thermocatalytic reaction is subtracted, the rate under photoirradiation becomes almost constant in the region of the catalyst concentration above 0.4 × 10⁻³ mol cm⁻³. This is due to the situation that incident photons are absorbed almost completely by the catalyst species in that region. The magnitude of its molar extinction coefficient (ϵ *ca.* 1.0 × 10⁴ at 254 nm) and the optical path length of the photoreactor (*ca.* 0.4 cm) support this view.

Figure 3 confirms that the rate of the photocatalytic reaction is first order with respect to the amount of incident

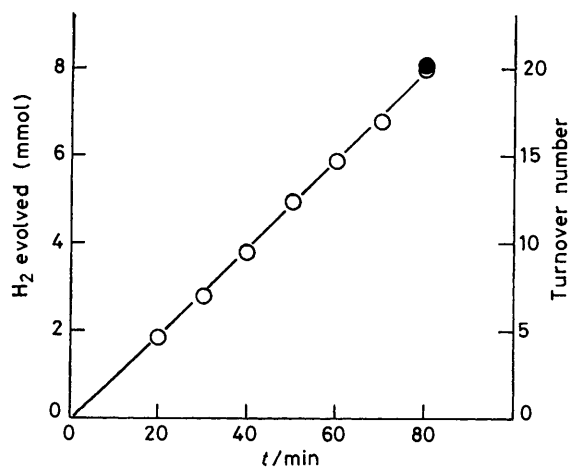


FIGURE 1 Time course of hydrogen formation (○) in the dehydrogenation of propan-2-ol under photoirradiation with low-pressure mercury lamps (82.5 °C). Catalyst composition: $\text{RhCl}_3 \cdot 3\text{H}_2\text{O}$ (2.0 mmol dm^{-3}), $\text{SnCl}_2 \cdot 2\text{H}_2\text{O}$ (10.0 mmol dm^{-3}), LiCl (5.9 mmol dm^{-3}). ● refers to the amount of acetone formed, analysed after the reaction

photons. The contribution from the thermocatalytic reaction is manifested in the intercept to the axis, while the slope reflects the efficiency of photoirradiation. The catalyst composition thus influences both the intercept and the slope.

With the increase in the added amount of $\text{SnCl}_2 \cdot 2\text{H}_2\text{O}$, the reaction rate was decreased under both photoirradiated and

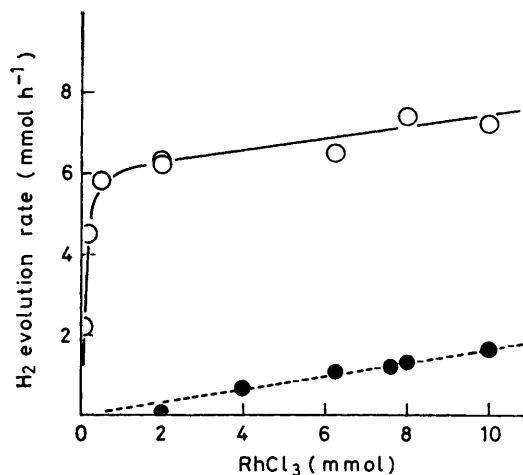


FIGURE 2 Dependence of the rate of photocatalytic (○) and thermocatalytic (●) reactions on the concentration of rhodium-tin complexes (82.5 °C). The ratios of $[\text{SnCl}_2] : [\text{RhCl}_3]$ and $[\text{LiCl}] : [\text{RhCl}_3]$ are fixed as 3.5 and 3.0, respectively

unirradiated conditions (Figure 4). The dependence is, however, far steeper in the latter than in the former.

Fourier transform ^{119}Sn n.m.r. measurements of the reaction solutions (each *ca.* 100-fold concentrated) disclosed that unco-ordinated Sn^{II} species became detectable only when the $[\text{SnCl}_2] : [\text{RhCl}_3]$ ratio reached *ca.* 6. The complete loss of thermocatalytic activity in the region $[\text{SnCl}_2] : [\text{RhCl}_3] \geq 6$ (Figure 4) may indicate that thermocatalytic reaction is strongly inhibited by unco-ordinated Sn^{II} species in the solution.

We have shown previously¹⁰ that ^{119}Sn n.m.r. spectro-

scopy is especially suited to characterize *in situ* the rhodium-tin complexes formed in aqueous hydrochloric acid solutions of $\text{RhCl}_3 \cdot 3\text{H}_2\text{O}$ and $\text{SnCl}_2 \cdot 2\text{H}_2\text{O}$. The relative intensities of ^{117}Sn satellite peaks definitely assist the identification of the series of $[\text{Rh}(\text{SnCl}_3)_n\text{Cl}_{6-n}]^{3-}$ ($n = 1-5$) complexes as well

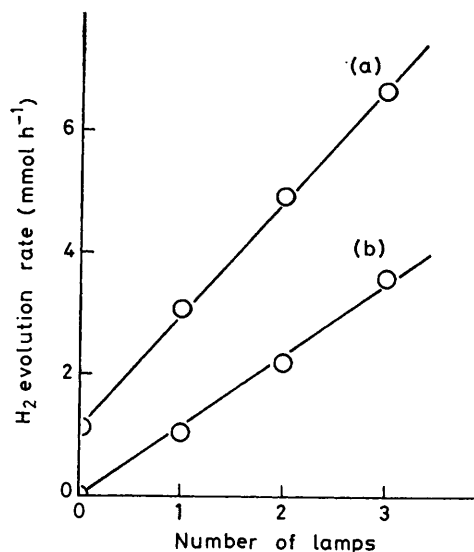


FIGURE 3 Dependence of the rate of photocatalytic reaction on the number of low-pressure mercury lamps (82.5 °C). Catalyst composition: (a) $\text{RhCl}_3 \cdot 3\text{H}_2\text{O}$ (6.25 mmol dm^{-3}), $\text{SnCl}_2 \cdot 2\text{H}_2\text{O}$ (22.19 mmol dm^{-3}), LiCl (18.44 mmol dm^{-3}), and (b) $\text{RhCl}_3 \cdot 3\text{H}_2\text{O}$ (2.0 mmol dm^{-3}), $\text{SnCl}_2 \cdot 2\text{H}_2\text{O}$ (20.0 mmol dm^{-3}), LiCl (5.9 mmol dm^{-3})

as the rhodium(I) complex $[\text{Rh}(\text{SnCl}_3)_5]^{4-}$. The Rh-Sn coordination bond is so strong that exchange between the SnCl_3^- ligands and the unco-ordinated Sn^{II} species is very slow on the n.m.r. time scale for rhodium(II)-tin(II) complexes, although the intramolecular rearrangement of the SnCl_3^- ligands occurs rapidly at 25 °C. In the series of Rh^{III} complexes $[\text{Rh}(\text{SnCl}_3)_n\text{Cl}_{6-n}]^{3-}$ ($n = 1-5$), the ^{119}Sn n.m.r. resonance is deshielded with concomitant decrease of $1/J(^{103}\text{Rh}-^{119}\text{Sn})$, as the number of tin ligands is increased.

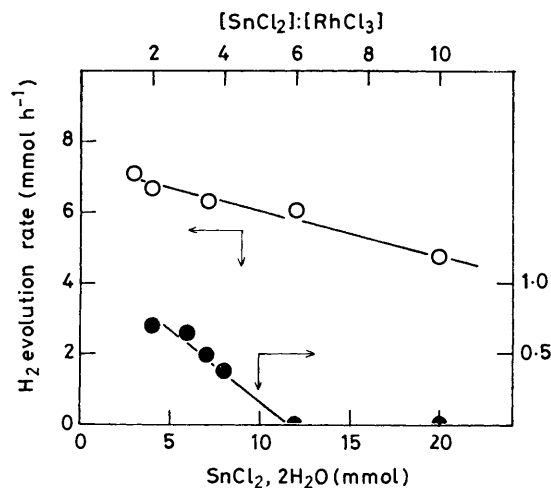


FIGURE 4 Dependence of the reaction rate on the added amount of $\text{SnCl}_2 \cdot 2\text{H}_2\text{O}$ under photoirradiated (○) and unirradiated (●) conditions (82.5 °C). The propan-2-ol solutions (200 ml) contain 0.40 mmol $\text{RhCl}_3 \cdot 3\text{H}_2\text{O}$ and 1.18 mmol LiCl

Thus a smooth curve is obtained from a plot of $^1J(^{103}\text{Rh}-^{119}\text{Sn})$ versus the ^{119}Sn chemical shift.¹⁰

Figure 5 displays representative ^{119}Sn n.m.r. spectra of the reaction solutions, which were removed at intervals after interrupting the thermocatalytic and photocatalytic reactions ($\text{RhCl}_3 \cdot 3\text{H}_2\text{O}$ 8.0 mmol dm⁻³, $\text{SnCl}_2 \cdot 2\text{H}_2\text{O}$ 24.0 mmol dm⁻³, LiCl 48.0 mmol dm⁻³) and concentrated *in*

changed simultaneously, there was observed a range in which the rate was almost constant (Table 2, runs 5–10). As revealed in the ^{119}Sn n.m.r. spectra, the solution composition is not simple. However, the reaction rate increased regularly with the proton concentration (Table 2, runs 11–13), where the amounts of tin(II) ion and total chloride ion were kept constant.

TABLE 1

Tin-119 n.m.r. characteristics of rhodium-tin complexes formed in propan-2-ol solutions of $\text{RhCl}_3 \cdot 3\text{H}_2\text{O}$, $\text{SnCl}_2 \cdot 2\text{H}_2\text{O}$, and LiCl

Complex	δ^a (p.p.m.)	$^1J(^{103}\text{Rh}-^{119}\text{Sn})/$ Hz	$^2J(^{117}\text{Sn}-^{119}\text{Sn})/$ Hz	$I(\text{satellite}):I(\text{main})$ (%) ^b	Number of tin ligands	Remark on structure
(1)	-52.2	523	1 682	15.1 (16.3)	5	<i>d</i>
(2)	-208.3	581	<i>c</i>	<i>c</i>	4	$[\text{Rh}(\text{SnCl}_3)_4\text{Cl}_2]^{3-}$ ^e
(3)	-113.1	557	1 917	12.3 (12.3)	4	<i>d</i>
(4)	-15.2	600	1 924	11.5 (12.3)	4	Hydride complex ^f
(5)	-426.4	742	2 847	7.6 (8.2)	3	$[\text{Rh}(\text{SnCl}_3)_3\text{Cl}_3]^{3-}$ ^g
(6)	-214.3	620	2 188	7.3 (8.2)	3	<i>d</i>
(7)	-276.0	679	2 216	<i>c</i>	2	<i>d</i>

^a Relative to external $\text{Sn}(\text{CH}_3)_4$ reference. ^b Values in parentheses are calculated statistically, based on the magnetic equivalence of tin ligands due to their fast intramolecular scrambling (*cf.* ref. 10). ^c Uncertain. ^d Structure unassigned. ^e δ -204.3 p.p.m., 1J 590 Hz, 2J 2 158 Hz in 3 mol dm⁻³ HCl solution. ^f $^2J(^{119}\text{Sn}-^1\text{H})$ 58.1 Hz. ^g δ -411.1 p.p.m., 1J 718 Hz, 2J 2 804 Hz in 3 mol dm⁻³ HCl solution.

vacuo. It is seen in both of the cases that there exist more than six kinds of rhodium-tin complexes, and that uncoordinated Sn^{II} or Sn^{IV} species are hardly detected. The presence of a hydride complex is obvious from the spectral change by proton decoupling [$^2J(^1\text{H}-^{119}\text{Sn})$ 58.1 Hz; Figures 5(b) and (c)], and was supported by ^1H n.m.r. spectra [$\delta_{\text{H}} - 12.0$, $^1J(^{103}\text{Rh}-^1\text{H})$ 9.8 Hz, $^2J(^{119}\text{Sn}-^1\text{H})$ 58.1 Hz]. It is to be noted that this hydride complex was not observed in the solution before the reaction. Table 1 summarizes the rhodium-tin complexes found in the ^{119}Sn n.m.r. spectra as major peaks. For all of them the oxidation number of rhodium was taken to be 3, because the plot of $^1J(^{103}\text{Rh}-^{119}\text{Sn})$ versus ^{119}Sn chemical shift of each complex fell upon the curve obtained for $[\text{Rh}(\text{SnCl}_3)_n\text{Cl}_{6-n}]^{3-}$ series.¹⁰ Complex (1) (δ -52.2 p.p.m. in Table 1) was detected only when the solution was measured before the reaction. The composition is affected not only by the ratios of $[\text{SnCl}_2]:[\text{RhCl}_3]$ and $[\text{LiCl}]:[\text{SnCl}_2]$ but also by pretreatment of the solutions.

A maximum was observed for the variation in the rate of the photoirradiated reaction with the added amount of lithium chloride (Table 2, runs 1–4). When the added amounts of tin(II) chloride and lithium chloride were

The temperature dependence of the reaction rates obtained under photoirradiated and unirradiated conditions are shown in Figure 6. The activation energy under the irradiated condition for the solution ($\text{RhCl}_3 \cdot 3\text{H}_2\text{O}$ 2.0 mmol dm⁻³, $\text{SnCl}_2 \cdot 2\text{H}_2\text{O}$ 3.0 mmol dm⁻³, LiCl 6.0 mmol dm⁻³) was 117 kJ mol⁻¹, the magnitude of which is reasonable compared with that for the transfer-dehydrogenation of propan-2-ol (89.5 kJ mol⁻¹).¹¹ It is noticeable that photoirradiation markedly reduced the activation energy to as low as 10.9 kJ mol⁻¹. Virtually the same value (10.7 kJ mol⁻¹) was obtained for a different catalyst composition ($\text{RhCl}_3 \cdot 3\text{H}_2\text{O}$ 2.0 mmol dm⁻³, $\text{SnCl}_2 \cdot 2\text{H}_2\text{O}$ 7.1 mmol dm⁻³, LiCl 5.9 mmol dm⁻³).

The colour of the reaction solution changed from wine-red to dark brown upon photoirradiation or by simple heating. Once changed, the colour was the same throughout the reaction. No reversion to the original was observed, even after photoirradiation, and the solution was cooled to measure the absorption spectra.

A typical electronic absorption spectrum of the dark brown solution is given in Figure 7. Three major absorption bands were observed. The intense u.v. absorption [peak (i), λ_{max} 208 nm, ϵ 29 500] may be assigned to a

TABLE 2

Variation of the photocatalytic reaction rate of propan-2-ol dehydrogenation with the concentration of added substances^a

Run	$[\text{SnCl}_2 \cdot 2\text{H}_2\text{O}]$ mmol dm ⁻³	$[\text{LiCl}]$ mmol dm ⁻³	$[\text{HCl}]$ mmol dm ⁻³	$[\text{H}_2\text{O}]$ mmol dm ⁻³	Rate H_2 mmol h ⁻¹
1	3.0	3.0	0.0	12.0	6.05
2	3.0	5.9	0.0	12.0	7.15
3	3.0	8.0	0.0	12.0	6.75
4	3.0	10.0	0.0	12.0	6.27
5	5.0	5.0	0.0	16.0	6.68
6	8.0	8.0	0.0	22.0	5.28
7	10.0	10.0	0.0	26.0	5.41
8	14.0	14.0	0.0	34.0	5.30
9	20.0	20.0	0.0	46.0	5.22
10	40.0	40.0	0.0	86.0	3.54
11	7.1	60.0	0.0	131.2	3.11
12	7.1	30.0	30.0	131.2	4.29
13	7.1	0.0	60.0	131.2	5.09

^a The concentration of $\text{RhCl}_3 \cdot 3\text{H}_2\text{O}$ is fixed as 2 mmol dm⁻³.

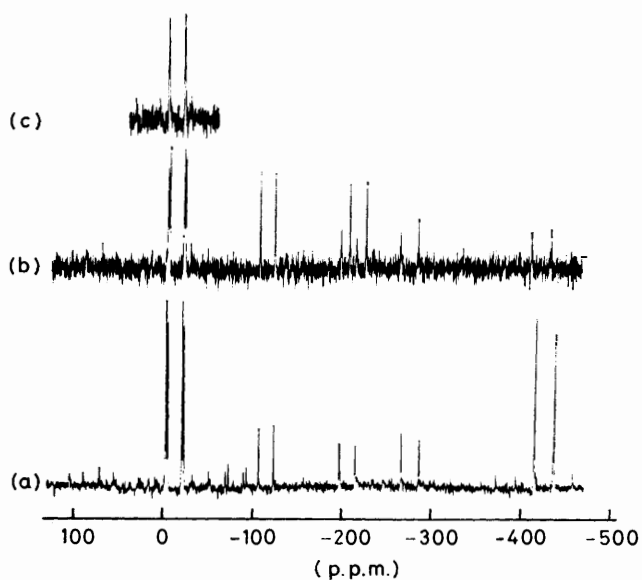


FIGURE 5 ^{119}Sn N.M.R. spectra of the solutions taken out by interrupting the thermocatalytic (a) and photocatalytic (b) reactions, and concentrated. The spectrum (c) shows the change of the spectrum (b) with proton noise-decoupling. Catalyst composition: $\text{RhCl}_3 \cdot 3\text{H}_2\text{O}$ (8.0 mmol dm^{-3}), $\text{SnCl}_2 \cdot 2\text{H}_2\text{O}$ ($24.0 \text{ mmol dm}^{-3}$), LiCl ($48.0 \text{ mmol dm}^{-3}$)

$\text{Rh}(d_\pi) \rightarrow \text{Sn}(\pi^*)$ charge transfer (CT) transition, since SnCl_3^- is known to be a strong π -accepting ligand,¹² and moreover it is absent without the addition of $\text{SnCl}_2 \cdot 2\text{H}_2\text{O}$. The medium peak around 280 nm [peak (ii)], which is superposed on peak (i), is assigned to a ligand \rightarrow metal

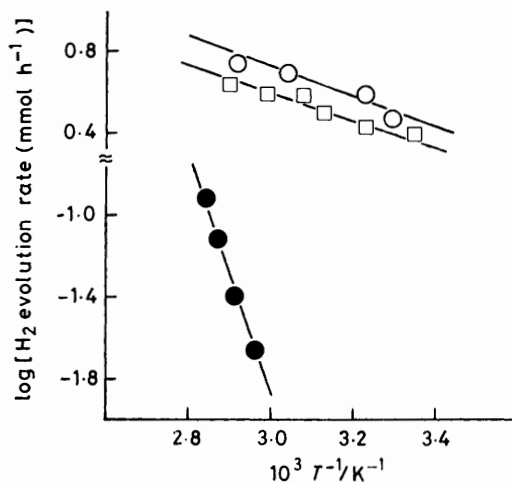


FIGURE 6 Temperature dependence of the reaction rate under photoirradiated (\circ, \square) and unirradiated (\bullet) conditions. Catalyst composition: \circ, \bullet , $\text{RhCl}_3 \cdot 3\text{H}_2\text{O}$ (2.0 mmol dm^{-3}), $\text{SnCl}_2 \cdot 2\text{H}_2\text{O}$ (3.0 mmol dm^{-3}), LiCl (6.0 mmol dm^{-3}); \square , $\text{RhCl}_3 \cdot 3\text{H}_2\text{O}$ (2.0 mmol dm^{-3}), $\text{SnCl}_2 \cdot 2\text{H}_2\text{O}$ (7.1 mmol dm^{-3}), LiCl (5.9 mmol dm^{-3})

CT transition (e.g., $\text{Cl} \rightarrow \text{Rh}$), on the basis of the peak assignment for RuCl_6^{3-} ¹³ and the fact that a similar band is present in the spectrum of RhCl_6^{3-} .¹⁴ A weak broad peak below ca. 400 nm [peak (iii)] would consist of $d-d$ transitions of various rhodium complexes in solution.

In Figure 7, the dependence of quantum efficiency on the wavelength is also shown.

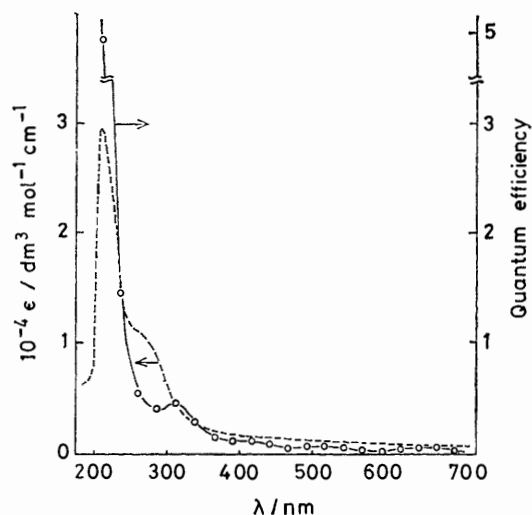


FIGURE 7 Wavelength dependence of quantum efficiency (20°C) and electronic absorption spectrum of the solution measured by interrupting the photocatalytic reaction (50 fold diluted). Catalyst composition: $\text{RhCl}_3 \cdot 3\text{H}_2\text{O}$ (2.0 mmol dm^{-3}), $\text{SnCl}_2 \cdot 2\text{H}_2\text{O}$ (7.1 mmol dm^{-3}), LiCl (5.9 mmol dm^{-3})

DISCUSSION

Mechanism of the Photoenhancement of the Reaction.—

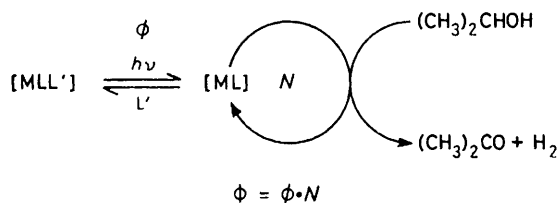
It is clear from Figure 7 that high quantum efficiency is obtained by photoirradiation around the wavelength of peak (i), exceeding unity at 20°C . Based on the temperature dependence of the reaction rate (10.9 kJ mol^{-1}), the quantum efficiency at 254 nm, the wavelength of the main emission band from the low-pressure mercury lamp, was estimated as 2.2 at the refluxing temperature (82.5°C).

For the photoaquation of Zeise's anion, in which the ethylene ligand is replaced by a water molecule,¹⁵ the $\text{Pt}(d_\pi) \rightarrow \text{ethylene}(\pi^*)$ CT excitation is claimed to be specifically effective because the π^* orbital is antibonding with respect to the platinum-ethylene bond.¹⁶ Recently Jaenicke *et al.* suggested that the $\text{Fe}(d_\pi) \rightarrow \text{CO}(\pi^*)$ excited state predominantly led to CO dissociation in the photolysis of (diene)tricarboxyliron.¹⁷ It is, therefore, conceivable that the $\text{Rh}(d_\pi) \rightarrow \text{Sn}(\pi^*)$ excited state brings about the dissociative loss of a SnCl_3^- ligand, generating a co-ordinatively unsaturated and hence catalytically active species.

Photoirradiation at the wavelength of peak (ii) is less effective as reflected in the wavelength dependence of quantum efficiency. For ligand \rightarrow metal CT excitation, the reduction of the central metal atom is often accompanied, and actually precipitation of metallic rhodium was observed around this peak with a certain catalyst composition.

It is of interest that the photoirradiation is also effective with visible light. As far as the implication of photoirradiation exists in the photodissociation of the ligand, it is reasonable that the photocatalysis proceeds in the $d-d$ region¹⁸ around peak (iii), although the quantum efficiency is low [e.g., Φ 0.03 (590 nm) at 20°C].

In accord with the above assumption, the mechanism for the photoenhancement of the present catalytic reaction is given in the Scheme. The catalytically active species ($[ML]$) is formed from the catalyst species ($[MLL']$) by photon absorption,¹⁹ and then incorporated



SCHEME $[MLL']$ = Catalyst species; $[ML]$ = catalytically active species generated by the ligand dissociation; Φ , quantum efficiency of the overall reaction; ϕ , quantum yield of the photodissociation of the ligand L' ; N , turnover number of the dehydrogenation cycle

into the catalytic cycle to dehydrogenate propan-2-ol. The cycle is repeated until $[ML]$ is turned back to $[MLL']$ by the re-coordination of the dissociated ligand L' . The re-coordination process should be rather fast, since no residual photocatalytic activity was observed after photoirradiation was turned off.⁸ The entire recovery of photocatalytic activity upon reillumination suggests that no irreversible process exists in the photoreaction of the catalyst species.

Incorporation of a hydride complex in the dehydrogenation cycle is assumed, since the effect of the proton concentration on the reaction rate (Table 2) corresponds to the reaction of a proton with the hydride ligand. The direct observation of a hydride complex will support this view, even if it is not itself involved in the cycle.

With this scheme, the quantum efficiency of the overall reaction is equal to the product of the quantum yield of the ligand-dissociating photoprocess (ϕ) and a turnover number of the dehydrogenation cycle (N). Thus a value of the quantum efficiency (Φ) larger than unity is expected, although ϕ cannot exceed unity theoretically. A high reaction rate may be provided by a high steady-state concentration of $[ML]$ under photoirradiation, while the low activation energy (*ca.* 11 kJ mol⁻¹) is associated with a quite low temperature dependence for the photoprocess. The fact of weaker rate dependence on the $[\text{SnCl}_2] : [\text{RhCl}_3]$ ratio under photoirradiation (Figure 4) indicates that the efficiency of photoexcitation differs little among the various rhodium-tin complexes.

Consideration from the Aspect of Chemical Storage of Solar Energy.—Thermal energy at low temperature is abundantly and easily supplied from suitable solar collectors or from waste energy in industrial plants. By combining the endothermic reaction (1) with an auxiliary operation such as gas compression or any product separation procedure (*e.g.*, distillation), it is possible to obtain the high temperature level heat by operating the reverse (exothermic) reaction at an elevated temperature. A chemical heat pump^{20,21} can thus be

assembled with this system. In fact, a propan-2-ol-acetone-hydrogen chemical heat pump, raising the temperature level from 55 to 160 °C, has been proposed recently.²²

However, the rate of reaction (1), associated with its endothermic character, is rather slow: *e.g.*, for homogeneous catalysts, turnover numbers (h⁻¹ at 82.5 °C) are 6 ($\text{RhCl}_3\text{-SnCl}_2$)⁹ and 13 $\{[\text{Ru}(\text{OCOCF}_3)_2(\text{CO})\text{-}(\text{PPh}_3)_2]\}$ ²³. The present photoenhanced rhodium-tin catalyst, attaining the turnover number of 88 h⁻¹ (82.5 °C), has substantiated the accelerating effect of photoirradiation. In addition, the reduction of the activation energy (117 \rightarrow 11 kJ mol⁻¹) will suppress the effect of temperature fluctuations in the heat source.

In order to utilize solar energy, it is important to compensate for its defects of diffuseness and intermittence. From this viewpoint, the following merits of the 'photoassisted chemical heat pump', proposed here, should be noted. (i) There is theoretically no limit in the quantum efficiency of reaction (1), as far as photoirradiation generates catalytically active species. (ii) The reactants in the reverse reaction of (1) (acetone and hydrogen) can be stored easily and stably, until the time when the high-temperature heat is demanded.

Improvements are, however, anticipated on the quantum efficiency in the visible wavelength region.

We are grateful to Dr. M. Suzuki of the National Research Laboratory for Pollution and Resources for the use of ¹¹⁹Sn n.m.r. facilities and to Professor S. Shiraishi, this Institute, for the spectrophotometric reactor. This work was supported by a Grant-in-aid from the Ministry of Education of Japan.

[1/1262 Received, 10th August, 1981]

REFERENCES

- R. J. Kazlauskas and M. S. Wrighton, *J. Am. Chem. Soc.*, 1980, **102**, 1727.
- G. L. Swartz and R. J. Clark, *Inorg. Chem.*, 1980, **19**, 3191.
- E. Samuel, *J. Organomet. Chem.*, 1980, **198**, C65.
- M. A. Schroeder and M. S. Wrighton, *J. Am. Chem. Soc.*, 1976, **98**, 551.
- J. C. Mitchener and M. S. Wrighton, *J. Am. Chem. Soc.*, 1981, **103**, 975.
- C. K. Grätzel and M. Grätzel, *J. Am. Chem. Soc.*, 1979, **101**, 7741.
- K. Chandrasekaran and D. G. Whitten, *J. Am. Chem. Soc.*, 1980, **102**, 5119.
- S. Shinoda, H. Moriyama, Y. Kise, and Y. Saito, *J. Chem. Soc., Chem. Commun.*, 1978, 348.
- (a) H. B. Charman, *J. Chem. Soc. B*, 1970, 584; (b) W. Strohmeier, E. Hitzel, and B. Kraft, *J. Mol. Catal.*, 1977-78, **3**, 61.
- H. Moriyama, T. Aoki, S. Shinoda, and Y. Saito, *J. Chem. Soc., Dalton Trans.*, 1981, 639.
- H. Imai, T. Nishiguchi, and K. Fukuzumi, *J. Org. Chem.*, 1974, **39**, 1622.
- J. F. Young, *Adv. Inorg. Chem. Radiochem.*, 1968, **11**, 91.
- P. K. Mehrotra and P. T. Manoharan, *Chem. Phys. Lett.*, 1976, **39**, 194.
- C. K. Jørgensen, *Acta Chem. Scand.*, 1956, **10**, 500.
- P. Natarajan and A. W. Adamson, *J. Am. Chem. Soc.*, 1971, **93**, 5599.
- N. Rösch, R. P. Messmer, and K. H. Johnson, *J. Am. Chem. Soc.*, 1974, **96**, 3855.

¹⁷ O. Jaenicke, R. C. Kerber, P. Kirsch, E. A. Koerner von Gustorf, and R. Rumin, *J. Organomet. Chem.*, 1980, **187**, 361.

¹⁸ A. W. Adamson and P. D. Fleishauer, 'Concepts of Inorganic Photochemistry,' Wiley, New York, 1975.

¹⁹ A. D. King, Jr., R. B. King, and E. L. Sillers, III, *J. Am. Chem. Soc.*, 1981, **103**, 1867.

²⁰ S. Fujii, H. Kameyama, K. Yoshida, and D. Kunii, *J. Chem. Eng. Jpn.*, 1977, **10**, 224.

²¹ W. M. Raldow and W. E. Wentworth, *Solar Energy*, 1979, **23**, 75.

²² M. Prevost and R. Bugarel, Proc. Int. Seminar on Thermochemical Energy Storage, Stockholm, 1980, p. 95.

²³ A. Dobson and S. D. Robinson, *Inorg. Chem.*, 1977, **16**, 137.